CONTENTS

CHAPTER 5

SOME WELL KNOWN SOURCES

CHAPTER 5

SOME WELL KNOWN SOURCES

In the last chapter we discussed some of the large scale features in the sky. In this chapter we wish to make some remarks on some of the well known sources which are resolved in our survey. We feel that a comparison of our maps with the published ones at a nearby frequency as well as those made at other frequencies will tell us something about the quality of our maps and their calibration. In choosing these sources we have restricted ourselves to those which have been earlier observed with the same telescope but in the single beam mode (except The Vela supernova remnant). To recall, the 'single beam mode' refers to the configuration wherein the combined outputs of the EW array and the S array are multiplied in a single channel analog receiver system. A sequential scanning of a maximum of 16 declinations of interest was employed in this mode (Sastry et al. 1981).

For the purposes of comparison with the earlier observations of these sources we have plotted our maps to approximately the same size as those of the earlier ones. However, in presenting the synthesis maps of these sources, we have deliberately shown the surrounding regions so that the noise level in the map can be clearly seen. The contour labels and the arrows on the contours have the same meaning as described in Chapter 4. However, an additional contour, corresponding to the average value between any two successive contour levels plotted in the maps given in Chapter 4, is given in the maps presented here for the purposes of comparison with the earlier observations.

Unless otherwise specified, the errors on the fluxes of sources obtained in the present survey are 8% (1σ). This error corresponds to the statistical uncertainty in the fluxes of point sources and includes the uncertainity in the estimation of background as well as day to day variation.

In this chapter spectral index, α , is defined in the sense flux $\propto$ frequency$^{\alpha}$.

5.1 THE CYGNUS LOOP

This is a well known supernova remnant (SNR) $\approx$ 20000 yr old, at a distance of $\approx$700 pc. It has an angular diameter of $\approx 3^{\circ}$, has both X-ray and optical counterparts (for a compilation of references to observations available on Cygnus Loop, see Green 1988 and references therein). This SNR has been observed over a wide range of radio frequencies.

Figure 5.1 shows the map of Cygnus Loop obtained by us. The next figure (Fig. 5.2) shows the map at 25 MHz obtained with the UTR2 telescope (Abranin et al. 1977). As may be seen there is good overall agreement between the two maps made at nearby frequencies and with similar resolution. In particular the minimum between the region C and the rest of the loop in the UTR2 map is seen very clearly in our maps also. It nay be worth pointing out that this region of minimum is characterised by the absence of $H\alpha$ emission (Hester et al. 1983) and X-ray emission (Rappaport et al. 1979). The total flux from Cygnus Loop obtained by integrating over the source in our synthesis map is 1100 Jy.

There has been some controversy regarding whether the radio emission from the region C (Fig. 5.2) is thermal or non-thermal.

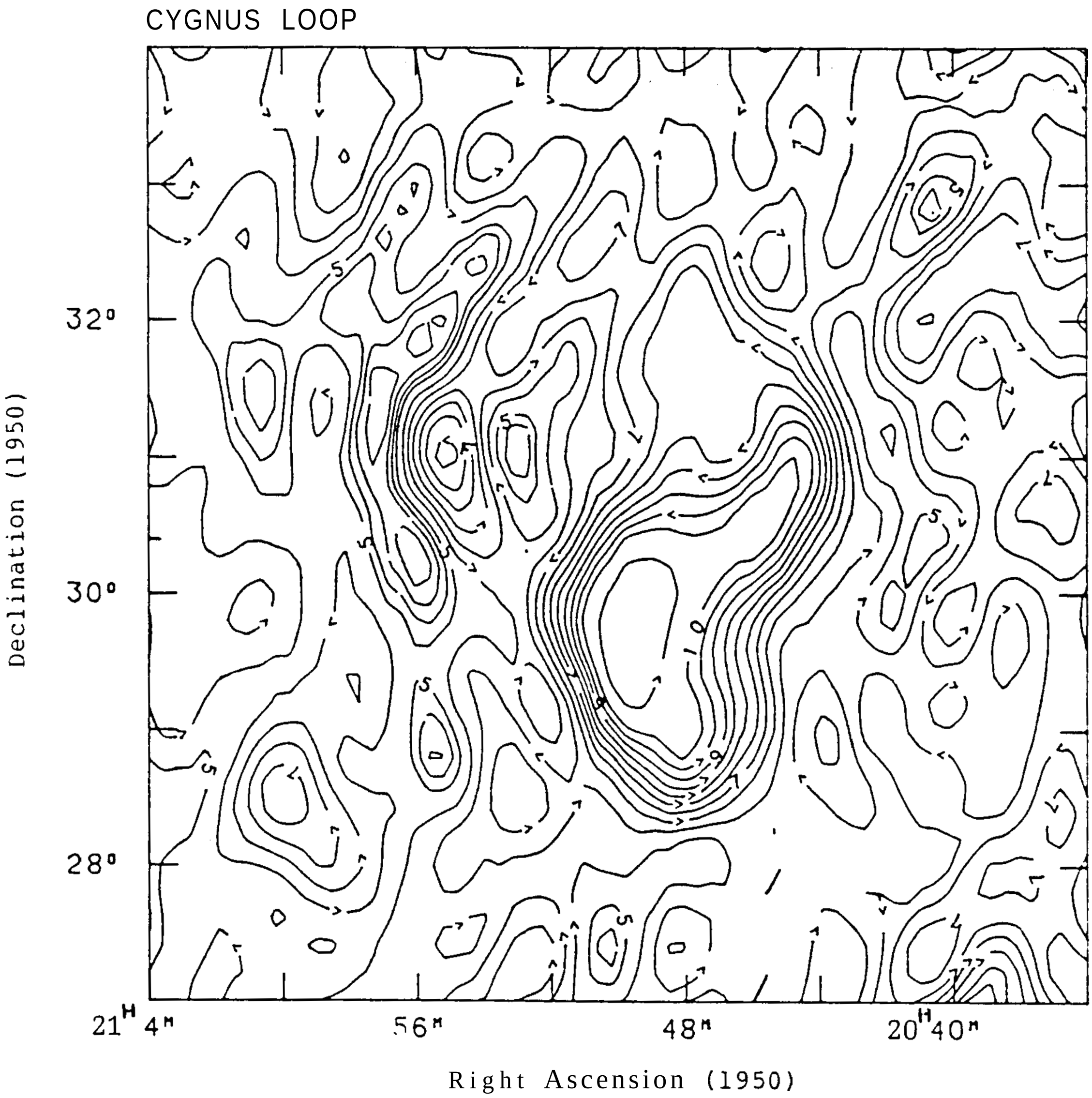

Fig. 5.1: Map of the Cygnus Loop made from the present survey. Contour labels are in units of 5722K of brightness temperature or 13 Jy/beam.

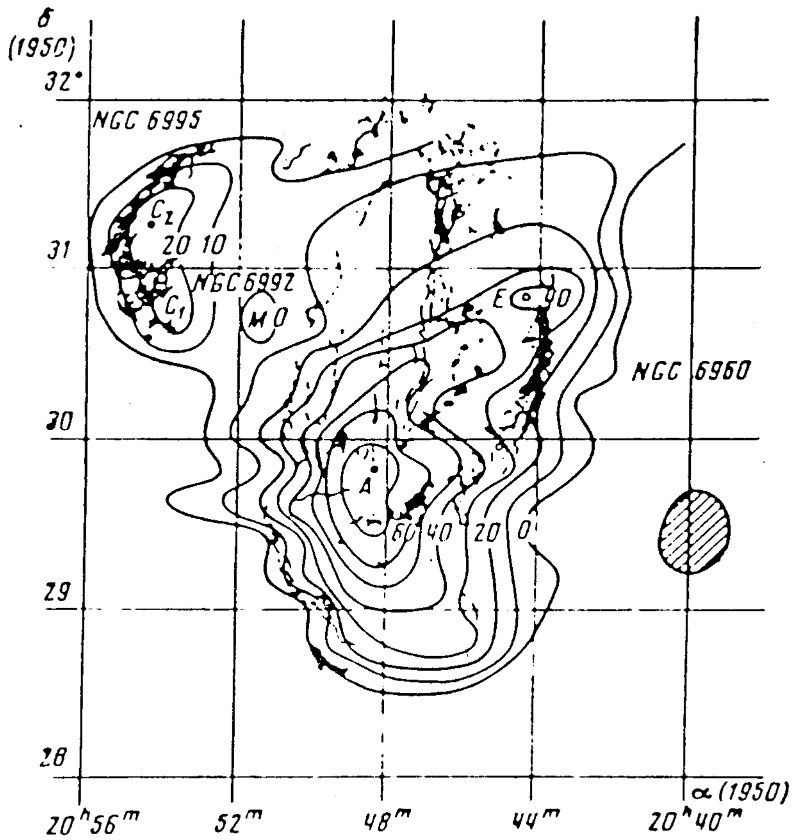

Fig. 5.2: Map of the Cygnus Loop at 25 MHz from Abranin et al. (1977). The numbers on the contours are in Jy/beam. The Hα photograph is superimposed on the radio picture.

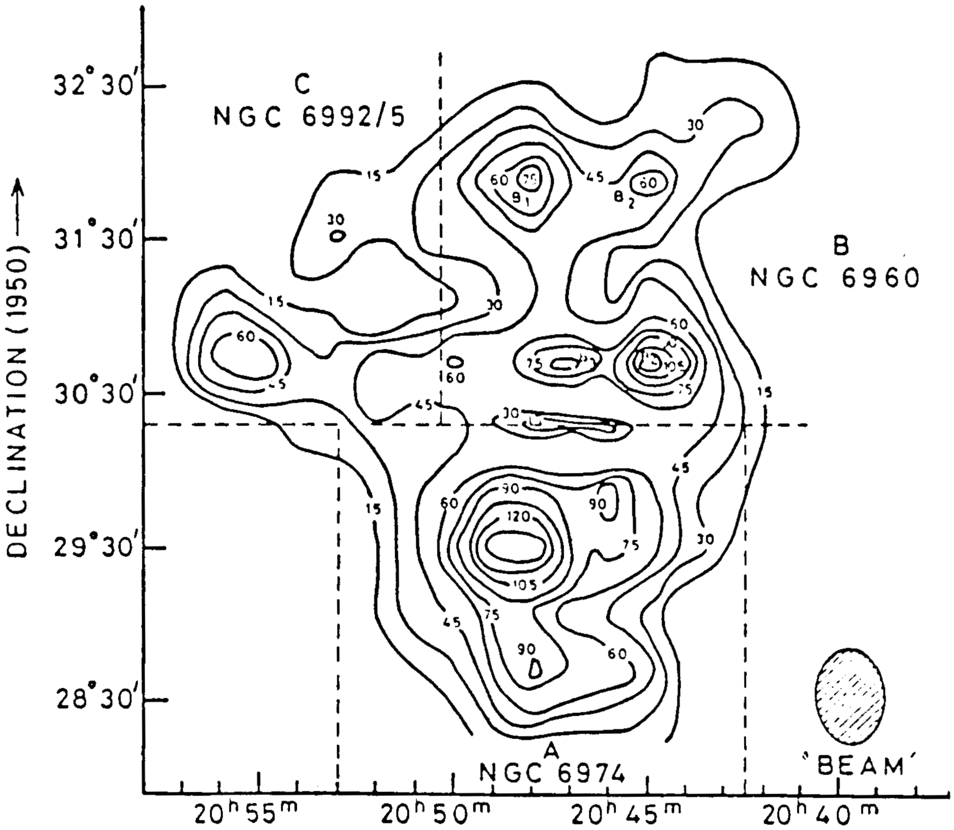

Fig. 5.3: Map of the Cygnus Loop at 34.5 MHz **from** Sastry et al. (1981). The numbers on the contours are in units of Jy/beam.

The reason for this controversy was the flat spectral index (0.0 below 400 MHz) deduced by Kundu and Velusamy (1967); this conclusion relied heavily on the 38 MHz flux of the region C obtained by Kenderdine (1963). The integrated flux from this region obtained from the present map (≈120 Jy) yields a steeper spectrum (-0.24 ± 0.1) than that obtained by Kundu and Velusamy (1967). We thus conclude that the radio emission from region C is also non-thermal in origin as the rest of the Loop.

Since there is a published map of Cygnus Loop obtained using the same telescope but in the single beam mode (Sastry et al. 1981) we felt that it would be appropriate to include this map also and make a couple of remarks. The single beam map shown in Fig. 5.3 suggests the presence of a number of compact emission regions such as B1,B2,B3 and B4. From a comparison with the synthesis map (Fig. 5.1) as well as maps made at other frequencies we conclude that the discrete features seen in the single beam map are probably due to (a) the calibration errors in the declination scans that were put together to produce the map and (b) the sidelobes of Cygnus A. But, the integrated flux obtained from the single beam map agrees with the present estimate within errors.

5.2 THE W51 COMPLEX

The map of the region surrounding W 51 obtained in the present survey is shown in Fig. 5.4(a). The map of the same region observed in the single beam mode (Deshpande and Sastry 1986) is given in Fig. 5.4(b). The absorption seen around 19^h20^m and $+13^\circ.5$ in the single beam map is also seen in the synthesis

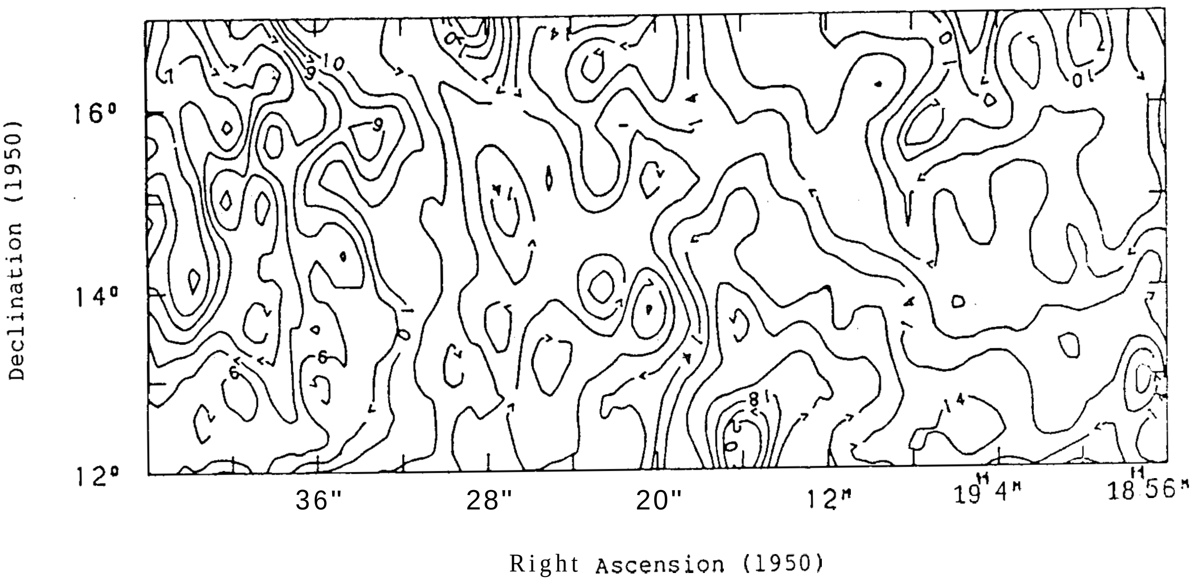

Fig. 5.4(a): Map of the W51 region made from the present survey.

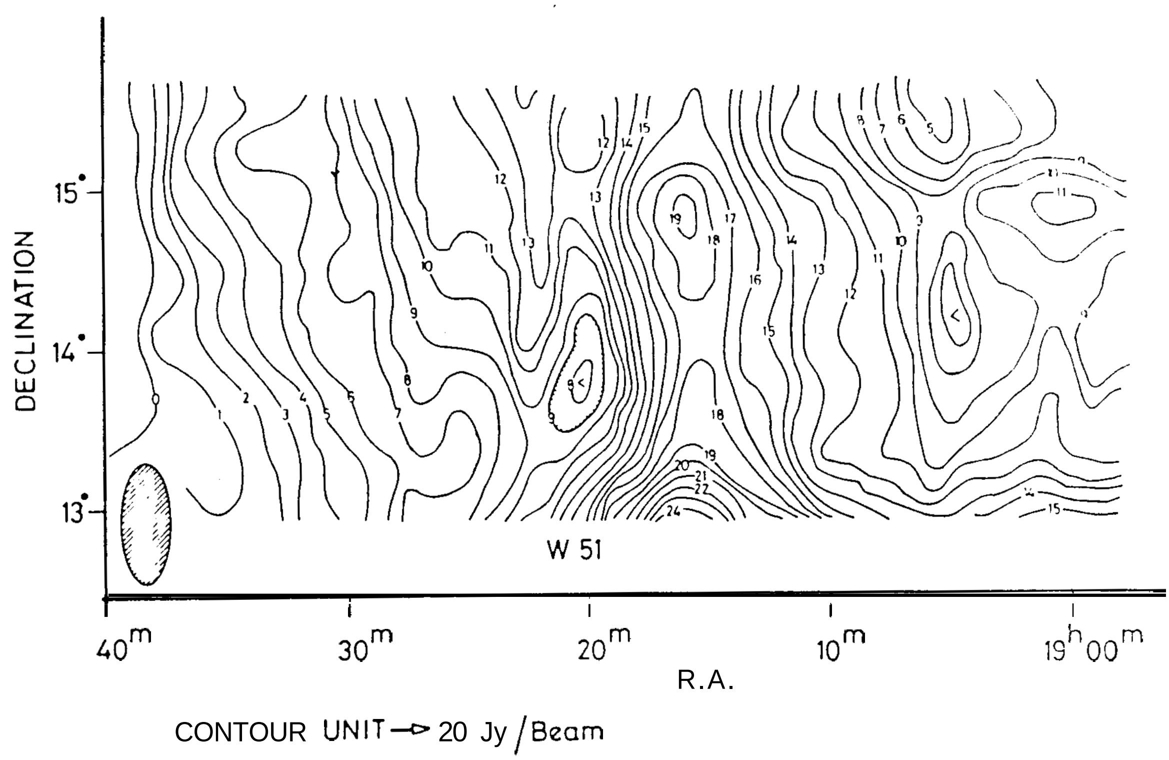

Fig. 5.4(b): Map of the W51 region made in the single beam mode from Deshpande and Sastry (1986).

Table 5.1 Fluxes of the 4 major groups of sources in W51. Errors on the 34.5 MHz fluxes are 8 % or 4 Jy (1σ) whichever is larger. 408 MHz fluxes are from Shaver(1969)

Source	α (1950) h m s	δ(1950) d m	Observed flux at 34.5 MHz (Jy)	Flux at 408 MHz (Jy)	Extrapolated flux at 34.5 (Jy)
W 51 A	19 21 30	+ 14 25	-72	61	128
W 51 B	19 20 30	+ 14 00	-81	31	65
W 51 C	19 18 00	+ 13 50	-1	18	38
W 51 E-arm	19 21 30	+ 13 50	-49	-	-

map. But, instead of the extended emission seen towards the south-east of this source in the single beam map, there is extended absorption in the synthesis map in this region. The strong emission source seen around $19^h 16^m$ and $+12^\circ.3$ is seen only partly in the single beam map. The other local maxima and minima seen in the single beam map are not seen in the synthesis map. We believe that the differences may be due to the fact that the sidelobes of strong sources such as Cygnus A (which are actually outside the region observed) were not cleaned in the single beam map.

<u>The Nature of W 51</u> : This is a complex region with many sources whose nature is uncertain (Terzian and Balick 1969). This region has been mapped at various frequencies - with a resolution of 2.8 at 408 MHz (Shaver 1969) and with a resolution of $2'.6$ at 4.875 GHz (Altenhoff et al. 1978) to quote two observations. The poorer resolution at low frequencies precludes any detailed study of this region based on our map. For example, Shaver identifies at least 8 discrete sources within one square degree. We can only get about 6 independent points in this region. However, some qualitative remarks on the nature of some of these sources can be made with the help of the 34.5 MHz observations. Table 5.1 lists the fluxes contained within one beam area centered at the positions indicated. Although, the beams overlap the trend indicated by the fluxes is clear. Even with a spectral index of -0.3 the extrapolated fluxes of all the sources are beyond 5σ and they should have been seen in <u>emission</u>. From the fact that they are not, one can conclude that there is. fairly strong

absorption in the foreground. Alternatively, the sources could be thermal.

5.3 HB 9 and IC 443

HB 9 is a supernova remnant believed to be at a distance of 1.8 kpc (Caswell and Lerche 1979) and its angular extent is about $2^\circ.5$. Its optical counterpart is a faint nebulosity marking the periphery of the remnant. Soft X-ray observations of the nebula by Touhy et al. (1979) indicate an age of 15,000 yr.

IC 443 is a shell-type supernova remnant with the optical counterpart similar to the radio shell. It is thought to be at a distance of 1.5 kpc (Duin and van der Laan 1975). X-ray observations by Parkes et al. (1977) indicate an age of approximately 12,000 yr for this remnant.

Observations with the Gauribidanur telescope using the single beam system have been reported by Dwarakanath et al. (1982 ; refered to as paper I in this section) for both these sources.

Fig. 5.5(a) and Fig. 5.5(b) show the maps containing HB 9 made in the synthesis mode and in the single beam mode respectively. They appear very similar. The integrated flux from HB 9 in Fig. 5.5(a) gives 700 Jy which is very close to the value obtained in paper I (750 ± 150 Jy). The reason for the good agreement between the two maps for this source is due to the fact that there are no strong sources nearby this source (unlike in the earlier two examples given in this chapter). This also suggests that antenna based errors are not so detrimental to the single beam observations as the uncleaned sidelobes of strong

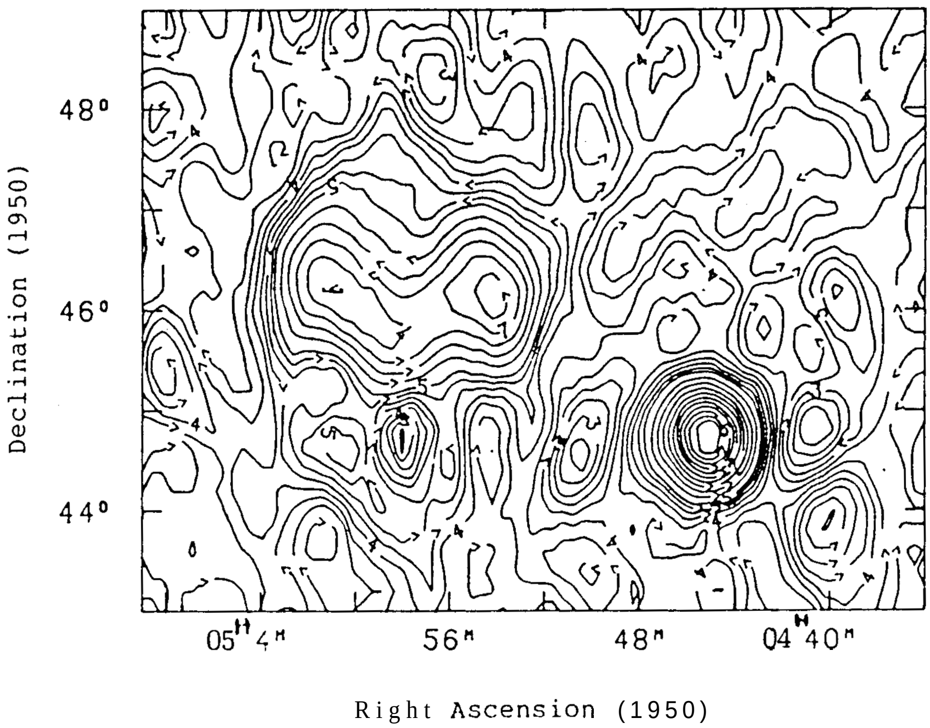

Fig. 5.5(a):. The supernova remnant HB9 as seen in the present survey. The strong source at the bottom right hand corner is 3C129+3C129.1.

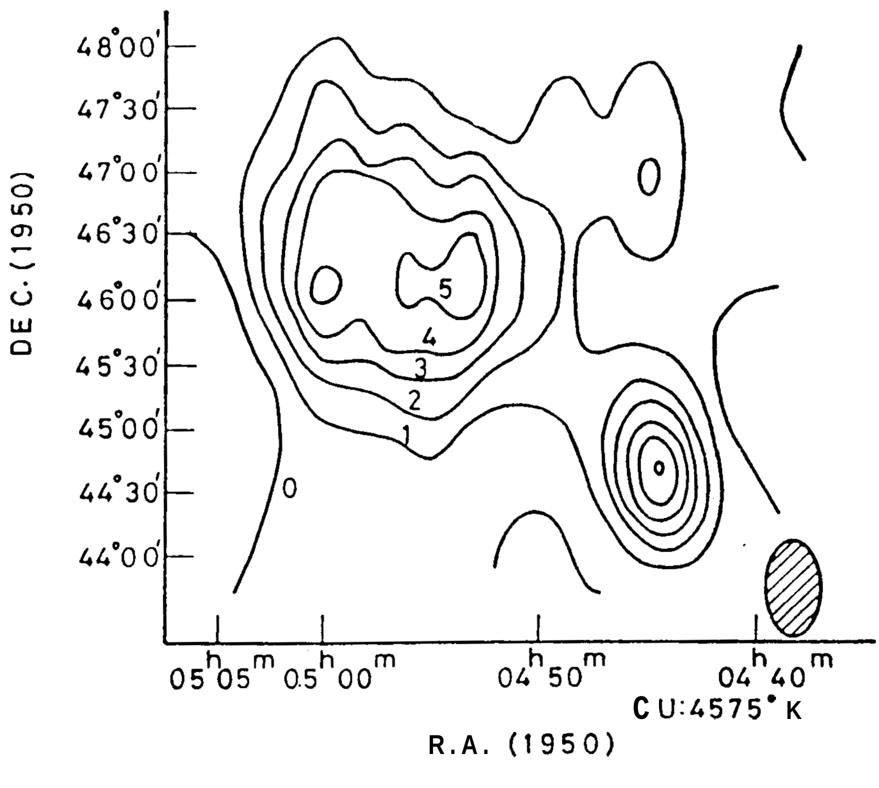

Fig. 5.5(b): HB9 mapped in the single beam mode of GEETEE by Dwarakanath et al. (1982).

sources.

The shell structure of IC 443 is unresolved by our beam. The observed half power widths are 42'x48' in R.A. and dec. implying 33'x29' for the size of the source in R.A. and dec. respectively. The integrated flux from IC 443 is 537 Jy compared to the earlier estimation of 440 ± 88 Jy in paper I. A detailed dicussion of the spectra of the two remnants can be found in paper I. All the conclusions reached there remain unaltered.

5.4 THE ROSETTE AND MONOCEROS NEBULOSITIES

The Rosette nebula has been observed over a wide range of frequencies (12 MHz to 4700 MHz). Above 400 MHz the spectrum of the nebula is -0.12 ± 0.05 consistent with optically thin thermal emission. Low frequency measurements have been combined with the 2700 MHz observations to derive an electron temperature of about 4100 K for the Rosette nebula (Graham et al. 1982).

Monoceros has also been observed over a wide range of frequencies from 111 MHz to 2700 MHz. Its spectrum fits a power law in this range with a spectral index of -0.47 ± 0.06. It is believed to be an SNR (Graham et al. 1982).

Fig. 5.6(a) shows a map containing the Rosette nebula obtained in the present survey. Rosette nebula is seen in absorption with an integrated flux density of -113 Jy. This agrees well with the previous observations done at other frequencies (Graham et al. 1982). Using our value and the 2700 MHz observation of Graham et al. (1982) we derive an average electron temperature (T_e) for the Rosette nebula of 5000 K. The two deeper absorptions seen on our map agree well in position

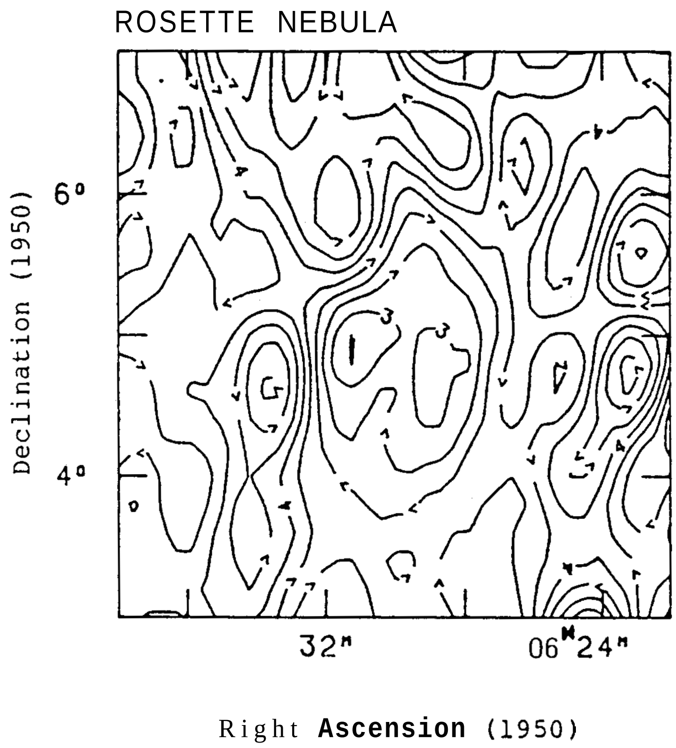

Fig. 5.6(a): Rosette nebula seen in absorption in the present survey.

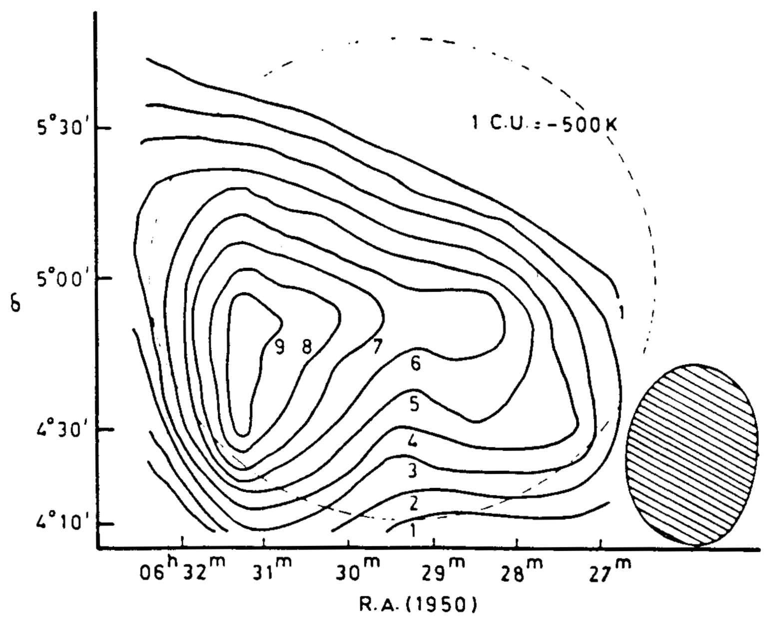

Fig. 5.6(b): Rosette nebula observed in the single beam mode of GEETEE (Deshpande et al. (1984)). .

with the two strong emission regions in the Rosette nebula seen in the 2700 MHz map (Graham et al. 1982) and the 408 MHz map (Shaver and Goss 1970).

The single beam observations of this source (Fig. 5.6(b)) at 34.5 MHz have been reported by Deshpande et al. (1984). There is a general agreement between the two maps. They obtain an integrated flux of -96 $\pm$19 Jy. The average T_e obtained by these authors is 5450$\pm$910 K. Both these numbers are in good agreement with our estimates. However, they make a strong point about the variation of T_e across the nebula - increasing from about 5000 K in the south-eastern region to about 8000 K in the north-western region based on their observations and the observation at 2700 MHz of Graham et al. (1982). This may not be the case: The extent and the depth of absorption observed on their map is $\approx 1^{\circ}$ and -10 Jy. Given the resolution of their map of $21' \times 33'$ and the sensitivity of ≈ 1.2 Jy (1σ), the evidence for any true variation in the absorption across the nebula is marginal. In addition, the north of the Rosette nebula borders the Monoceros nebula which is seen in emission (Fig.5.7). This will certainly reduce the amount of absorption seen towards the north due to convolution effects.

The integrated flux from the Monoceros nebulosity (Fig. 5.7) after correcting for the point sources in the field of view is 134 Jy (The point sources in the field of view were taken from Graham et al. 1982, In those cases where spectral index was not mentioned, it was assumed to be -0.8). The flux expected at 34.5 MHz on the basis of its spectrum (-0.47$\pm$0.06) between 111 MHz and 2700 MHz is 794 Jy. Given the nature of the Monoceros

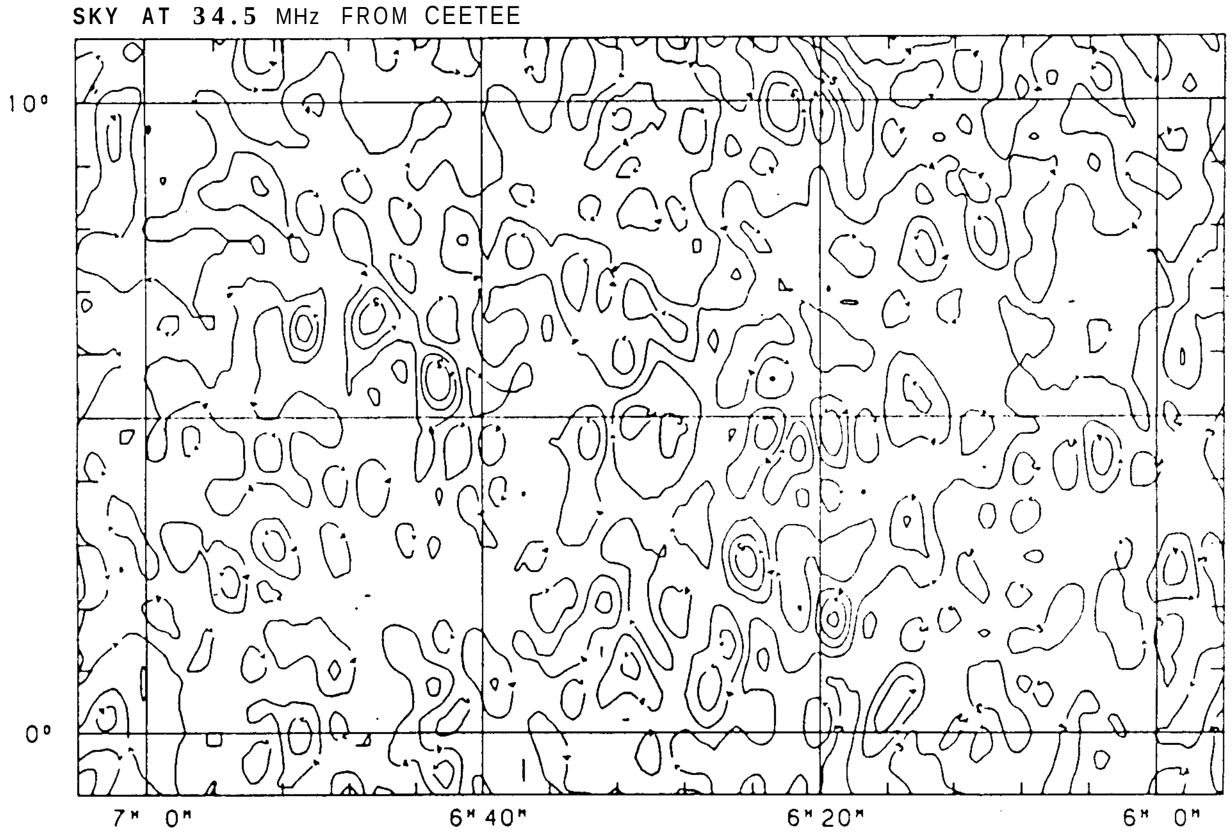

Fig. 5.7: Map of the region containing the Rosette nebula and the Monoceros nebula from the present survey.

nebulosity (Odegard 1986) this implies an external absorption of flux from the Monoceros nebula which in itself is a non-thermal source. A χ^2 fit to the observed fluxes of Monoceros nebula of the function

$$S_\nu = \frac{2k_B}{\lambda^2}(T_e - T_B)(1 - e^{-\tau})\,\Omega_{SNR} + S_{\nu,SNR}\, e^{-\tau} \qquad (5.1)$$

gives $\tau = 0.14$ and $T_e < 1000$ K (Fig. 5.8(a)). Here,

T_e is the electron temperature of the absorbing gas,

τ is the optical depth of the absorbing gas,

T_B is the background brightness temperature,

Ω_{SNR} is the solid angle of the SNR, and

$S_{\nu,SNR}$ is the expected flux of the SNR at the frequency ν.

It is interesting to note here that this absorbing gas is confined to the region of Monoceros nebulosity and not wide spread. This is evident from the measured fluxes of the sources G 207.1-1.3, G207.2+1.3, G207.3+1.1 and G206.9+2.3 on our maps which do not show any significant reduction in their fluxes from that expected from an extrapolation from higher frequency. It is very likely that this gas might be the outer regions of the Rosette nebula itself and if Monoceros nebula is behind the Rosette nebula it could very well be absorbed.

Nils Odegard (1986), in analysing the observations of Monoceros from Clark Lake in conjunction with high frequency continuum observations and Hα measurements in that direction concludes that so far as the region near $06^h 36^m$ and $+6^\circ 12'$ is concerned, there is evidence for a gas at $T_e \approx 8000$ K and EM ≈ 180 cm^{-6} pc. This gas has a $\tau = 0.09$ at 34.5 MHz. From our

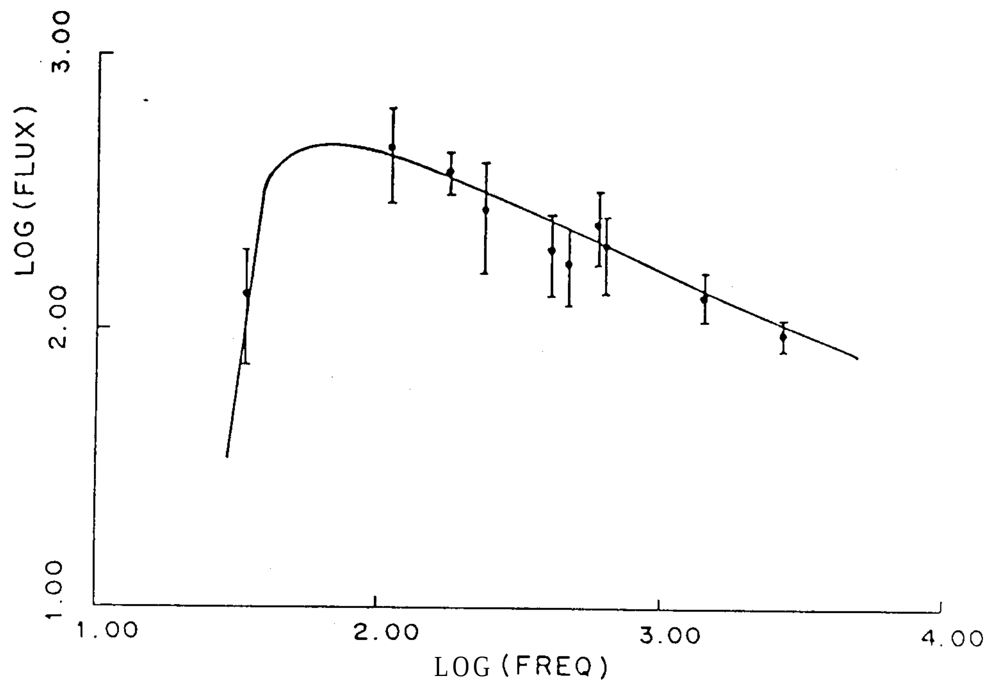

Fig. 5.8(a): Spectrum of the Monoceros nebulosity. The integrated flux at 34.5 MHz is from the present observation. Rest of the fluxes are taken from Graham et al. (1982). The solid line represents eq. (5.1) with τ =0.14 and T_e =1000 K.

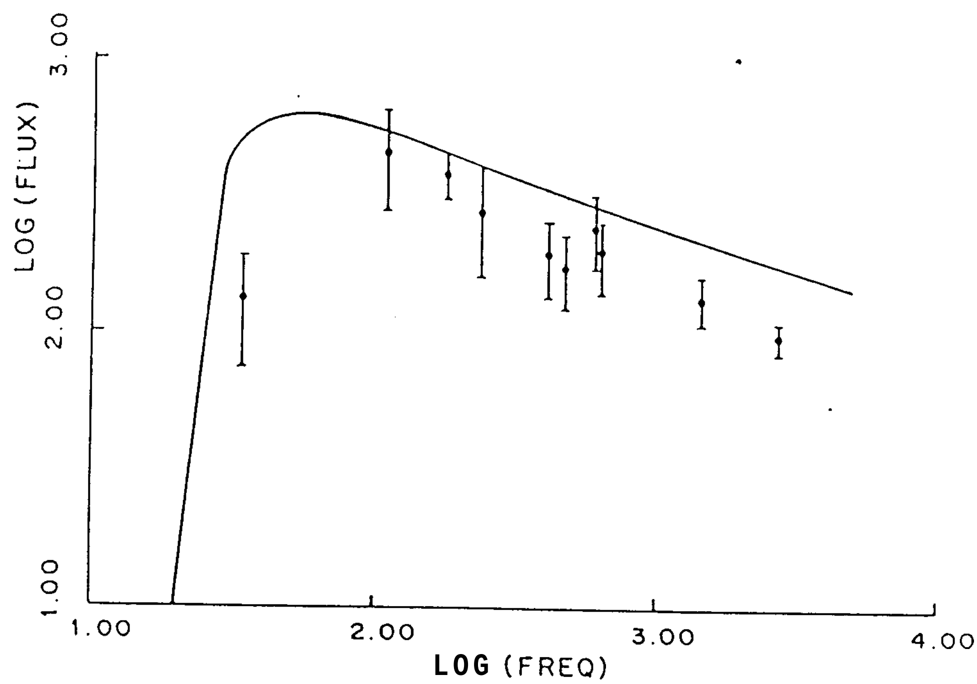

Fig. 5.8(b): Same as Fig. 5.8(a) **but** the solid line represents eq. (5.1) for τ =0.09 and T_e = 8000 K.

observations, it is evident that this gas is unlikely to be responsible for the absorption of the flux from Monoceros. The fit is very poor for T_e = 8000 K and τ = 0.09 as can be seen in figure 5.8(b). The fit is quite a sensitive function of τ though not so sensitive of T_e. Thus, if the gas is uniformly distributed, it has a τ = 0.14, $T_e \approx 1000$ K and an EM = 17 cm^{-6} pc. Of course, absorption in a gas of higher optical depth but lower filling factor can not be ruled out from the present analysis.

5.5 THE COMA CLUSTER

The diffuse radio emission from the Coma cluster of galaxies has been mapped in the range of 400 to 1400 MHz. (Hanisch 1980; Jaffe and Rudnick 1979). Figure 5.9(a) shows a map of the region including the Coma cluster obtained from the present observations. The observations at 34.5 MHz in the single beam mode have already been reported by Sastry and Shevgaonkar (1983). Fig. 5.9(b) shows a map of the Coma cluster region at 34.5 MHz reproduced from their paper. There is general agreement between the two maps.

Some measured and derived parameters of the two regions, Coma A and Coma C, are listed in Table 5.2. With a view to ascertaining the nature of a possible halo at 34.5 MHz around these two sources, their total fluxes and angular sizes were measured. While it is clear from the maps shown in figures 5.9(a) and 5.9 (b) that both Coma A and Coma C are extended, it is not immediately obvious whether it is .the effect of an extended halo or due to a combination of many unresolved sources. The 5C4 survey by Willson (1970) in the Coma Berenices area lists

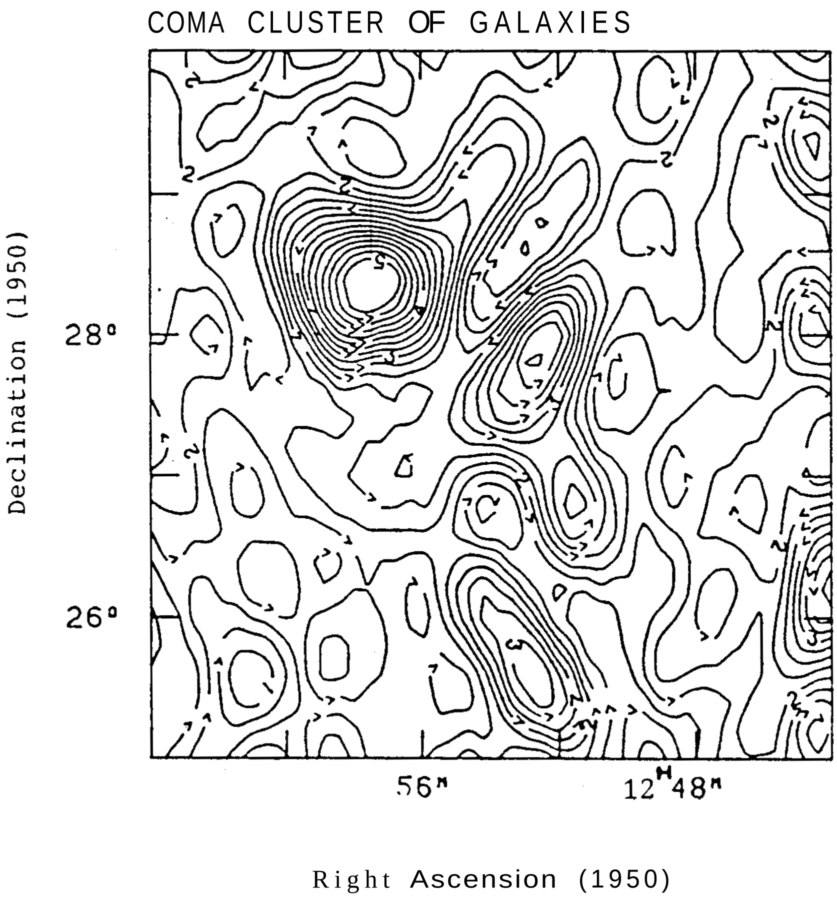

Fig. 5.9(a): Radio emission from the Coma cluster of galaxies mapped in the present survey. Contour interval is $\simeq$ 3 Jy/beam.

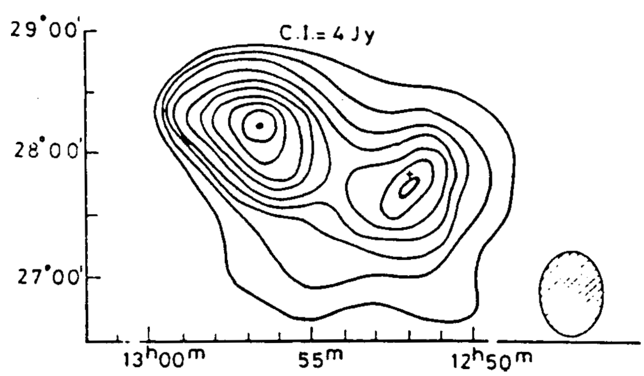

Fig. 5.9(b): Radio emission from the Coma cluster of galaxies mapped in the single beam mode of GEETEE (Sastry and Shevgaonkar (1983)).

Table 5.2 Some measured and estimated parameters of the diffuse radio emission from the Coma cluster of galaxies. Numbers in parantheses refer to measurements made at 408 MHz - those under Coma A by Ballarati et al.(1980) and under Coma C by Hanisch (1980).

	Coma A	coma C
Position	$12^h 52^m 40^s$ $+ 27^o 47'$	$12^h 57^m 20^s$ $+ 28^o 20'$
Measured source size (FWHM) (r.a. x dec.)	29'x53'	44'x49'
Derived source size	12'x36' (10'x22')	36'x31' (40'x41')
Position angle of major axis	120^o (125^o)	50^o ($40^o \pm 20^o$)
Total measured flux (Jy)	54	120
Total flux of halo (Jy)	15	80
Spectral index of halo	-1.0	-1.4

189 sources for all of which 408 MHz fluxes are available. Not all of them have identifications. The integrated flux of all the unresolved extragalactic sources in the Coma C area is about 40 Jy at 34.5 MHz (assuming a spectral index of -0.8). This still leaves 80 Jy unaccounted (see Table 5.2) which must come from a diffuse component which is resolved out in the 408 MHz interferometric observations. Hanisch (1980) has estimated the flux from the halo of Coma C to be 2.55 Jy at 430 MHz. This implies a spectal index of -1.4 between 430 and 34.5 MHz.

A similar analysis can be done for Coma A. All of the 54 Jy from the Coma A area can be accounted for by the integrated flux of the unresolved extragalactic sources in the Coma A area (3C 277.3 whose flux is 5844 mJy at 408 MHz, has been extrapolated to 34.5 MHz with a spectral index of -0.72 ; others have been extrapolated with -0.8). On the other hand, if only those sources in the Coma A area are taken which are identified with galaxies, then, their integrated and extrapolated flux will be 39 Jy, leaving about 15 Jy unaccounted. Given the uncertainties in all these estimates, the evidence is not compelling for a halo around Coma A at 34.5 MHz. Ballarati et al. (1981) estimate a flux of 1.18 Jy at 408 MHz for the diffuse emission near Coma A. Assuming 15 Jy for the diffuse emission flux at 34.5 MHz, this implies a spectral index of -1.0.

A true map of the diffuse emission or the halo can only be obtained by convolving the sources in Willson's (1970) list with the beam at 34.5 MHz and subtracting the 'synthesized map' from the present one.

5.6 THE VELA SUPERNOVA REMNANT

Vela (Vela XYZ) is a supernova remnant (Weiler 1983) at a distance of 0.5 kpc (Milne 1968). It has been studied in the radio, optical and X-rays (see Weiler and Panagia 1980 and references therein).

A map of the Vela region obtained by us is shown in Pig. 5.10. Vela X ($\alpha = 08^h 36^m\!.6$ $= -46^\circ$) is believed to be a plerion while Vela Y ($\alpha = 08^h 44^m\!.6$ $= -43^\circ$) and Vela Z ($\alpha = 08^h 48^m\!.$ $\delta = -46^\circ$) are thought to form part of a shell. Weiler and Panagia (1980) discuss the spectra of the remnants Vela X and Vela YZ separately and between 85 MHz and 5 GHz approximate them in the following form :

$$S_X(Jy) = 1115 \left(\frac{\nu}{GHz}\right)^{-0.08} \qquad (5.2)$$

$$S_{YZ}(Jy) = 650 \left(\frac{\nu}{GHz}\right)^{-0.65 \pm 0.22} \qquad (5.3)$$

One of the major reasons for classifying Vela X as a plerion is the flat spectral index of -0.08 (Weiler and Panagia 1980) as opposed to the spectral indices of typical shell-type remnants which are close to -0.45 (Clark and Caswell 1976).

Recently Milne and Manchester (1986) have raised doubts about Vela X being classified as a plerion. The major reason for their doubt is the fluxes used for the determination of the spectral index of Vela X by Weiler and Panagia (1980). We reproduce in Table 5.3 the fluxes used by Weiler and Panagia (1980) to determine the spectral index of Vela X.. From this it

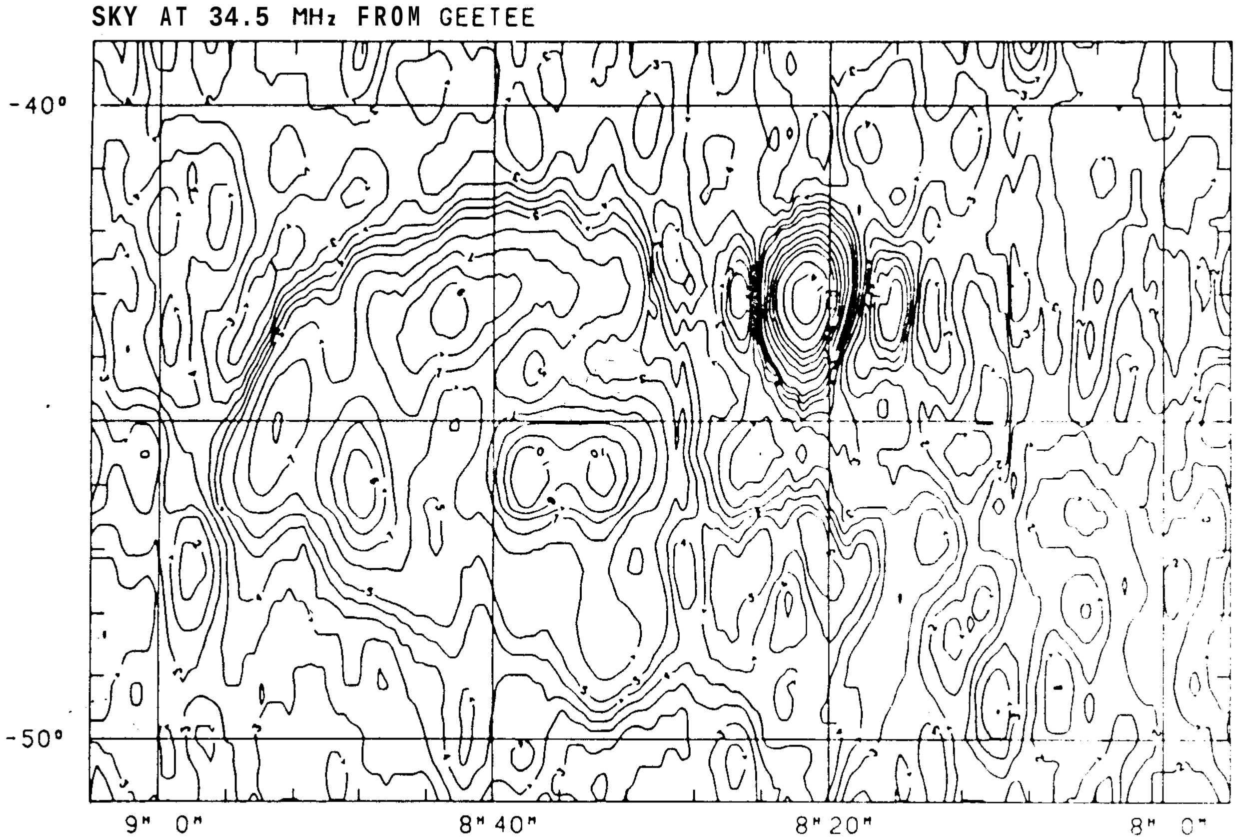

Fig. 5.10: The Vela supernova remnant mapped in the present survey. It extends from 08^h28^m to 08^h56^m and from -48^o to -41^o. The source around 08^h20^m, -43^o is Puppis A, another supernova remnant.

Table 5.3 Integrated fluxes of Vela X used by Weiler and Panagia (1980) to estimate the spectral index of Vela X to be −0.08. The expected flux at 34.5 MHz on the basis of this spectral index is 1459 Jy. The observed value is 1648 Jy

Frequency (GHz)	Flux (Jy)	Reference
0.0855	1600	Rishbeth (1958)
1.440	920	Mathewson et al. (1962)
2.700	1050	Milne (1980)
5.000	759	Milne (1980)

is evident that the 85 MHz value is crucial in estimating the spectral index. Milne and Manchester (1986) make this point, and claim that this flux may be affected by the free-free absorption occurring in the SNR itself or in the Gum nebula (although they give no specific arguments for this). In **additon,** they point out that the measurement of Vela X at 408 MHz and 635 MHz by Milne (1968) have been ignored in the estimate of the spectral index of Vela X by Weiler and Panagia (1980) which, if included, imply a spectral index of -0.3 to -0.4 for Vela X for frequencies above 635 MHz. If this is true, the argument for Vela X as a plerion weakens.

In order to clarify this, we have done two things:

(a) We have integrated our **maps** at 34.5 MHz shown in Fig. 5.10 to obtain fluxes of Vela X and Vela YZ. We obtain **values** of 1648 Jy and 3556 Jy respectively (the regions of integration are : for Vela X, $\alpha = 08^h 28^m$ to $08^h 41^m$ and $\delta = -44^\circ$ to -48°; for Vela YZ, $\alpha = 08^h 28^m$ to $08^h 56^m$ and $\delta = -41^\circ$ to -44° plus $\alpha = 08^h 41^m$ to $08^h 56^m$ and $\delta = -44^\circ$ to -48°). From equations 5.2 and 5.3 the expected fluxes at 34.5 MHz for Vela X and Vela YZ are 1459 Jy and 5798 Jy. There appears to be no absorption against Vela X. The 34.5 MHz flux of Vela X establishes the spectrum of Vela X more firmly at -0.08.

(b) In addition we have integrated the 635 MHz map of Milne (1968) to estimate a flux for Vela X. Assuming the total flux for the remnant Vela XYZ of 2360 Jy (Milne 1968) we obtain a flux for Vela X of 1211 Jy. The value expected **from** equation (5.2) is 1156 Jy.

As far as the **spectrum** of Vela YZ is concerned, the estimated flux at 34.5 MHz fits well with a spectral index of **-0.5** rather than **-0.65.** Since Vela X and Vela YZ are well separated on our maps, we believe that the integrated flux of Vela YZ determined by us is reliable. Since Vela X itself, which is more in line of sight with the Gum nebula, does not show any absorption at 34.5 MHz, it is unlikely that Vela YZ is affected by any absorption in the Gum nebula. So, we suggest a spectral index of **-0.5** for Vela **YZ** rather than a spectral index of -0.65.

REFERENCES

Abranin,E.P., Bazelyan,L.L., Goncharov,N.Yu. 1977, Sov. Astr., 21, 441.

Altenhoff,W.J., Downes,D., Pauls,T., Schraml,J. 1978, Astr. Astrophys. Suppl. Ser., 35, 23.

Ballarati,B., Feretti,L., Ficarra,A., Gavazzi,G., Giovannini,G., Nanni,M., Olori,M.C. 1981, Astr. Astrophys., 100, 323.

Caswell,J.L., Lerche,I. 1979, Mon. Not. R. astr. Soc., 187, 201.

Clark,D.H., Caswell,J.L. 1976, Mon. Not. R. astr. Soc., 174,267.

Deshpande,A.A., Sastry,Ch.V. 1986, Astr. Astrophys., 160, 129.

Deshpande,A.A., Shevgaonkar,R.K., Sastry,Ch.V. 1984, Astrophys. Space Sci., 102, 21.

Duin,R.M., van der Laan,H. 1975, Astr. Astrophys., 40, 111.

Dwarakanath,K.S., Shevgaonkar,R.K., Sastry,Ch.V. 1982, J. Astrophys. Astr., 3, 207.

Graham,D.A., Haslam,C.G.T., Salter,C.J., Wilson,W.E. 1982, Astr. Astrophys. 109, 145.

Green, D.A. 1988, Astrophys. Space Sci., 148, 3.

Hanisch,R.J. 1980, Astr. J., 85, 1565.

Hester, J.J., Parker, R.A.R., Dufour, R.J. 1983, Astrophys. J., 273, 219.

Jaffe,W.J., Rudnick,L. 1979, Astrophys. J., 233,453.

Kenderdine,S. 1963, Mon. Not. R. astr. Soc., 126, 55.

Kundu,M.R., Velusamy,T. 1967, Ann. d'Astrophysique, 30, 723.

Mathewson,D.S., Healey,J.R., Rome,J.M. 1962, Aust. J. Phys.,15,354.

Milne,D.K. 1968, Aust. J. Phys., 21, 201.

Milne,D.K. 1980, Astr. Astrophys., 81, 293.

Milne,D.K., Manchester,R.N. 1986, Astr. Astrophys., 167, 117.

Odegard,N. 1986, Astrophys. J., 301, 813.

Parkes,G.E., Charles,P.A., Culhane,J.L., Ives,J.C. 1977, Mon. Not. R. astr. Soc., 179, 55.

Rappaport, S., Petre, R., Kayat, M.A., Evans, K.D., Smith, G.C., Levine, A. 1979, Astrophys. J., 227, 285.

Rishbeth, H. 1958, Aust. J. Phys., 11, 550.

Sastry, Ch.V., Dwarakanath, K.S., Shevgaonkar, R.K. 1981, J. Astrophys. Astr., 2, 339.

Sastry, Ch.V., Shevgaonkar, R.K. 1983, J. Astrophys. Astr., 4, 47.

Shaver, P.A. 1969, Mon. Not. R. astr. Soc., 142, 273.

Shaver, P.A., Goss, W.M. 1970, Aust. J. Phys. Suppl., 14, 77.

Terzian, Y., Balick, B. 1969, Astr. J., 74, 76.

Tuohy, I.R., Clark, D.H., Garmine, G.P., 1979, Mon. Not. R. astr. Soc., 189, 59p.

Weiler, K.W. 1983, Supernova Remnants and their X-ray Emission, p.299 - 320, Eds. J.Danziger and P.Gorenstein.

Weiler, K.W., Panagia, N. 1980, Astr. Astrophys., 90, 269.

Willson, M.A.G. 1970, Mon. Not. R. astr. Soc., 151, 1.